

EFFECT OF GEAR POSITIONS ON AIRFIELD RIGID PAVEMENT CRITICAL STRESS
LOCATIONS

By:

Jeffery Roesler, Francisco Evangelista Jr, and Marcelo Domingues

Department of Civil and Environmental Engineering

University of Illinois at Urbana-Champaign

205 N. Mathews, MC-250

Urbana, IL 61801 USA

Phone: (217) 265-0218; Fax: (217) 333-1924

jroesler@uiuc.edu

fevange2@uiuc.edu

mduoming3@uiuc.edu

PRESENTED FOR THE
2007 FAA WORLDWIDE AIRPORT TECHNOLOGY TRANSFER CONFERENCE
Atlantic City, New Jersey, USA

April 2007

ABSTRACT

Airfield rigid pavement thickness design has been based on the critical tensile bending stress at the bottom of the slab. Recent observations from full-scale rigid pavement tests at the FAA's NAPTF and Airbus PEP have shown top-down cracking can occur under certain combined loading and pavement geometry configurations. Similar cracking modes have been seen in recent years under certain highway loading and slab situations. The objective of this paper is to identify key slab loading locations on airfield rigid pavements which alter the critical tensile bending stress in the concrete slab from being on the slab bottom to the top of the slab, given no initial curling. Five individual aircraft gear geometries (e.g., dual, dual tandems, triple dual tandems) and four main landing gear (e.g., B-777, A-380, MD-11, and B-747) analyses were conducted for a given slab configuration, pavement geometry, and materials. The numerical results show that the ratio between the top of the slab and bottom tensile stresses were significantly higher for the main landing gear analysis relative to the individual gear analysis. Furthermore, this initial finite element analysis has shown consideration of the entire main landing gear of the aircraft is necessary if the top tensile stresses are going to be accurately predicted.

INTRODUCTION

Airfield rigid pavement thickness design has traditionally been based on the critical tensile bending stress at the bottom of the slab. The Federal Aviation Administration (FAA) design guide for rigid pavements uses the Westergaard edge stress as the critical response for facilities without the triple dual tandem (TDT) gear aircraft. For designs considering TDT gear aircraft, a layered elastic analysis is employed which uses the greater of the interior stress or 75 percent of the free edge stress. Recent observations from full-scale rigid pavement tests at the FAA's National Airport Pavement Test Facility (NAPTF) and Airbus Pavement Experimental Program (PEP) have shown top-down cracking can occur under certain combined loading and pavement geometry situations (Brill et al. [1]; Fabre et al. [2]). Similar cracking modes have been seen in recent years under certain highway loading and slab configurations (Mahoney et al. [3]; Smith et al. [4]; Harvey et al. [5]; Heath and Roesler [6]; Beckemeyer et al. [7]). Finite element analysis has shown these alternative cracking modes, especially top-down cracking, primarily occur on highway slabs in the presence of built-in curling (Heath et al. [8]; Hiller and Roesler [9]; Rao and Roesler [10,11]).

National Airport Pavement Test Facility (NAPTF)

The NAPTF, located at the FAA Technical Center, in New Jersey, USA, conducted full-scale traffic testing of airfield rigid pavements. This testing effort is aimed at incorporating actual performance data into the new FAA pavement design procedure. Three Construction Cycle test sections (CC1, CC2, and CC3) have been constructed in the past 5 years with different testing objectives. The objectives of section CC2 was to compare the fatigue performance of concrete pavements under different support conditions and gear configurations (4- and 6-wheel gears). The CC2 tests occurred between April and December of 2004. Details about the construction, operation and testing procedures can be found in Hayhoe [12] and Brill et al. [1]. Several papers

published on the full-scale results pointed out the occurrence of top-down cracking in both the trafficked and non-trafficked lanes (Brill et al. [1]; Brill [13]; Guo [14]).

Brill et al. [1] observed top-down cracks in both outside and inside lanes of CC2 even though the slabs were reported to have minimal permanent curl (lift-off remained $\leq 0.38\text{mm}$). Both top-down and bottom-up crack patterns were observed on the inside traffic lanes (trafficked with 4- and 6-wheel gears) during repeated loading. The outside lane received trafficking from only the outer wheels of the gear and cracked in a top-down pattern, earlier than the inside lane. The authors suggested that this kind of cracks in the outside lanes were induced by the transfer of load through the dowelled joints.

Guo [14] also analyzed the results of several NAPTF tests (CC1 and CC2) and proposed consideration of both the environmental and traffic loading, since some level of initial or residual curling existed in the slab. This assumption was proposed to try to explain top-down cracking especially at the corners which has been reported by other authors to explain corner cracking developed during accelerated load testing of highway rigid pavements (Rao and Roesler [10]; Rao [15]). Guo [14] observed that top-down cracks occurred, even for thick slabs, in the longitudinal direction between the two transverse joints when both loaded gears moved near these joints. This pattern of cracks was also observed on the unloaded slabs. Guo [14] cited results from the CC1 testing in 2000 to show that the top-down patterns occurred when measured strains at the top were lower than the strains at the slab bottom. Guo [14] pointed out that some longitudinal cracks between consecutive transverse joints were observed after 28 gear passes before even corner cracks were noticed. He reported that the tensile stresses developed on the slab bottom were related primarily to the wheel load, while the tensile stresses on the slab top were related primarily to the gear load at both the longitudinal and transverse joint locations.

Airbus Pavement Experimental Program (PEP)

Full-scale rigid pavement tests, called A-380 Pavement Experimental Program (PEP-rigid phase), were investigated to determine the effects of materials (subgrade support), slab geometry (slab size, dowels, slab thickness), environment (thermal curling), and gear type on the response and fatigue life of the concrete pavement structures (Fabre et al. [2]; Fabre and Balay [16]). Top-down cracks were the predominant cracking pattern mainly along the slab's corners as well as the central longitudinal axis of the slab. Quasi-static tests (2 km/h) showed that the maximum strains were obtained close to the longitudinal joint as was also observed in NAPTF's tests. The study also pointed out that the A-380 gear positions were not more damaging than a B-747 or B-777 regardless of the thermal conditions. This fact was explained by the gear geometry of the A-380.

To explain the high percentage of top-down cracks at the PEP, indirect tension tests were performed on cores extracted from top and bottom of the slabs. The results indicated that the strength at the top could be 35 percent less than the bottom. Fabre and Balay [16] pointed out some contributing factors to this observation, such as paving efficiency, homogeneity of vibration, and uncontrolled drying of the top of the slab during concrete hardening. McCullough and Dossey [17] and Rao [15] also observed that the strength of concrete at the top of the slab can be less than strength at the bottom of the slab due to moisture loss (higher evaporation rates) experienced near the slab surface.

RESEARCH OBJECTIVES

This research study will identify key slab loading locations on airfield rigid pavements which induce the highest tensile stresses at the top and bottom of the slab given a flat slab condition. The 2-D finite element analysis program ILLISLAB (Khazanovich, [18]) was used for the initial analyses, but NIKE3D (3-D finite element analysis program) will be used for future numerical simulations and verification of the 2-D analyses. To quantify the slab response due to different load configurations and positions, tensile stresses were evaluated for each loading condition considering individual gear types (e.g., B-737, B-747, B-767, and B-777) and the main landing gears of four aircraft (e.g., A-380, B-777, B-747, and MD-11).

METHODOLOGY

Nine slabs each measuring 300 by 300 inches (25ft. x 25ft.) with a thickness of 16 in. were analyzed to determine the critical tensile locations under aircraft loading. Figure 1 presents the slab arrangement for the cases studied. The following inputs were assumed for all the cases analyzed:

- Concrete elastic properties: $E_c = 4.5 \times 10^6$ psi and $\nu = 0.15$
- Modulus of subgrade reaction: $k = 150$ psi/in
- Tire contact pressure: $p = 200$ psi
- Tire geometry: length = width = 15 in.
- Wheel load per tire: $P = 45,000$ lbs

The finite element analyses were divided into the following two cases:

Case I: The following individual gears were placed at 256 different positions on the central slab in Figure 1: B-737, B-747 (dual tandem), B-757 (dual tandem), B-767 (dual tandem), and B-777 (triple dual tandem). The axle and wheel spacing for each individual gear are described in Table 1. The loaded gear was also positioned across the transverse and longitudinal joints to determine if that position would cause critical tensile stresses. The deflection load transfer efficiency (LTE) across the transverse and longitudinal joints was assumed to be 85 percent ($LTE_x = LTE_y = 85\%$), which approximately represents a stress load transfer of 75 percent. The load transfer was simulated by aggregate interlock or shear only transfer.

Case II: All main landing gears for the A-380-800, B-747-400, B-777, and MD-11 aircraft were positioned as shown in Figure 1 so that all gears traversed the slab in both the x- and y-directions. Table 2 presents the spacing between the main landing gears and their individual gear dimensions. The Wing Landing Gear (WLG) spacing is the horizontal distance from the wing gear to the nearest body gear while the Body Landing Gear (BLG) spacing is the distance between the two body gears. The number of gear positions analyzed was different for each aircraft due to varying gear geometry and spacing. As an example, Figure 1 shows the positions

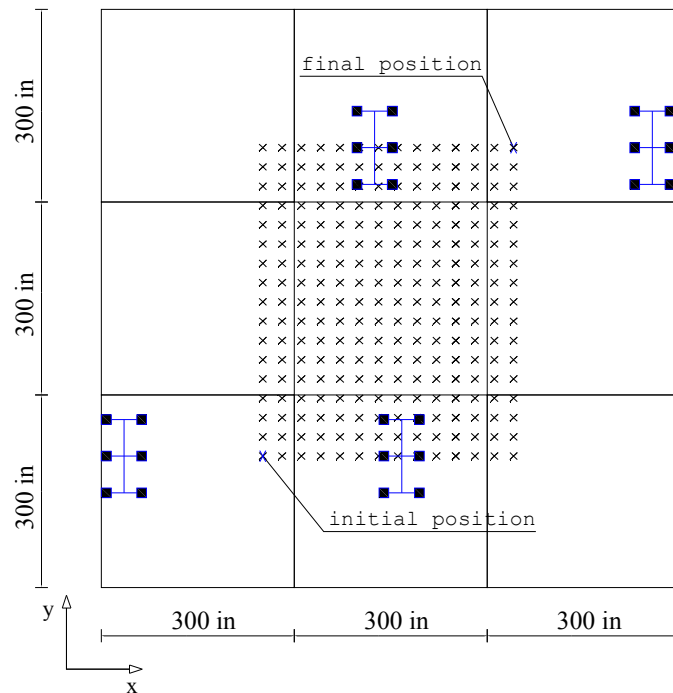


Figure 1. Slab geometry and load positions for the B-777 gears (Case II).

Table 1.
Wheel and axle spacing on each individual aircraft gear.

| Aircraft | Axle Spacing (in.) | Wheel Spacing (in.) |
|----------|--------------------|---------------------|
| B-737 | - | 30.5 |
| B-747 | 58.0 | 44.0 |
| B-757 | 45.0 | 34.0 |
| B-767 | 56.0 | 45.0 |
| B-777 | 57.0 | 55.0 |

Table 2.
Aircraft gear, axle, and wheel spacing.

| Aircraft | WLG spacing (in.) | BLG spacing (in.) | Axle spacing (in.) | Wheel spacing (in.) |
|-----------------------|-------------------|-------------------|--------------------|---------------------|
| A380-800 ^a | 141.6 | 207.2 | 67.0 ^b | 61.0 ^b |
| B747-400 | 141.0 | 151.0 | 58.0 | 44.0 |
| B777 | ^c | 432.0 | 57.0 | 55.0 |
| MD-11 | 210.1 | ^d | 64.0 | 54.0 |

^aThe dimensions were taken from Fabre et al. [2].

^bThese dimensions were used for the TDT. The values of 67.0 and 53 inches were used for the axle and wheel spacing on the wing landing gear, respectively.

^cThe B-777 does not have WLG.

^dThe MD-11 has a dual wheel belly gear with a wheel spacing of 37.4 in.

simulated for the B-777 gears, where the cross symbols represent the centerline of the two gear positions. As shown in Figure 1, the aircraft's main landing gears were positioned across the transverse and longitudinal joints with the LTE assumed to be either zero (free edge case) or 85 percent.

RESULTS AND DISCUSSION

Case I (Individual Gear Analysis)

Table 3 summarizes the results for the maximum tensile stresses (σ_{tx}^{MAX} and σ_{ty}^{MAX}) at the bottom and top of the central slab for the individual gear analyses (Case I) for all potential loading positions. The results in Table 3 are only valid for the specific gear geometry, gear load, and rigid pavement system assumptions in this paper. As expected, the maximum tensile stresses were on the bottom of the slab for all individual gear types. The maximum stress locations were approximately at the mid-slab edge, either at the transverse or longitudinal joint depending on the gear type. Due to its small wheel spacing, the B-737 produced the greatest tensile stress at the slab bottom (y-direction) for all gears analyzed. The largest top tensile stress came from the TDT gear (B-777) in the x-direction. The maximum tensile stress at the top was similar in the x- and y-direction for each gear type. The preliminary results confirmed Guo et al.[14] statement that the gear load affected the maximum tensile stress at the top of the slab while the wheel primarily affected the bottom slab tensile stresses.

In order to determine the likelihood of top-down cracking occurring relative to bottom-up cracking (without slab curling), the ratio between the top and bottom tensile stress for each gear type was calculated and presented in Table 3. The B-777 gear produced the highest ratio of 0.50. Since all the tensile stress ratios were small, it is unlikely that top-down cracking would occur before bottom-up cracking if only individual gear types are analyzed with a no curling assumption. Even if a reduced strength assumption is made for the surface zone concrete, the strength would have to be 50 percent of the bottom zone concrete which is improbable. The next step is then to simultaneously analyze all of the aircraft's main landing gears with the same slab and gear configuration assumptions to determine the potential for top-down tensile cracking.

Table 3.
Summary of the Maximum Tensile Stresses at the Top and Bottom of the Central Slab for an Individual Gear Loading ($LTE_X = LTE_Y = 85\%$).

| Individual Gear Type | σ_{tx}^{MAX} (psi) | | Top to Bottom σ_{tx}^{MAX} ratio | σ_{ty}^{MAX} (psi) | | Top to Bottom σ_{ty}^{MAX} ratio |
|----------------------|---------------------------|-------------|---|---------------------------|-------------|---|
| | Bottom | Top | | Bottom | Top | |
| B-737 | -379 | -153 | 0.40 | -484 | -159 | 0.33 |
| B-747 | -433 | -212 | 0.49 | -438 | -212 | 0.48 |
| B-757 | -456 | -206 | 0.45 | -439 | -198 | 0.45 |
| B-767 | -446 | -208 | 0.47 | -443 | -212 | 0.48 |
| B-777 | -462 | -231 | 0.50 | -405 | -201 | 0.50 |

Case II (Main Landing Gear Analysis)

Tables 4 and 5 present the maximum tensile stress values (σ_{tx}^{MAX} and σ_{ty}^{MAX}) at the bottom and top of the central slab for the main landing gear analysis given a joint LTE of either 0 or 85 percent, respectively. As the load transfer efficiency across the joints decreased for all aircraft types, the maximum tensile stresses at the top and bottom increased. The bold values in both tables represent the maximum tensile stress at the top of slab for each aircraft type. As expected, the maximum tensile stress is still at the bottom of the slab for each aircraft type, approximately at the mid-slab edge for the LTE of 0 percent and slightly closer to corners for an LTE of 85 percent. The maximum stresses at the bottom of the slab were either in the x- or y-direction depending on the aircraft type. The B-747 and MD-11 produced the greatest tensile stress on the bottom for the LTE of 0 percent, while the B-777 and MD-11 produced these highest values for the LTE of 85%. The main landing gears of the A-380 resulted in the highest top tensile stresses for both LTE values considered. For all aircraft types, the maximum tensile on the top of the slab was in the x-direction. This finding indicates that longitudinal cracking would be the most likely failure mode for this slab geometry and pavement layer properties.

The ratio between the top and bottom tensile stresses were also presented in Tables 4 and 5. The results were quite different than the individual gear results in Table 3. For LTE = 0%, 9 out of 10 ratios were greater than 0.50 for the x- and y-directions. In fact, the A-380 and MD-11 produced top-bottom tensile stress ratios in the x-direction around 1.0. For LTE = 85%, the top-bottom tensile stress ratios were smaller but still were significantly higher than the individual gear analysis in Table 3. The A-380 produced the greatest top-bottom tensile stress ratio for the high joint LTE. The top to bottom tensile stress ratio indicates that top-down cracking (especially longitudinal cracking) is plausible for several of the aircraft analyzed (B-747, A-380, and MD-11) for LTE close to zero. Note, the MD-11 and A-380 have significantly higher tensile stresses at the bottom of the slab in the y-direction compared to the top tensile stresses in the x-direction which could first lead to bottom-up transverse cracking. For high LTE, top-down cracking would likely occur only if there were significant strength reductions in the top zone of the concrete slab.

Assuming high joint load transfer, Tables 5 confirms what Fabre et al. [2] reported, that the dual tridem of the A-380 does not produce the highest response relative to the twin dual tandem of the B-747 and the MD-11 (see bottom stresses in the y-direction). However, for this analysis, the A-380 aircraft does produce a larger tensile stress at the top of slab relative to the B-747, B-777, and MD-11 (see top x-direction stresses in Table 5).

In order to visualize the slab stresses reported in Tables 4 and 5 due to different gear configurations and positions, the location and critical tensile stress (σ_{tx}^{MAX} or σ_{ty}^{MAX}) at the top of slab were plotted along with the position of the aircraft gears for that stress level. Figures 2 through 5 present the positions for the A-380, B-747, B-777, and MD-11, respectively. The cases of load and slab symmetry were omitted in the plots. In Figure 2, the A-380 is shown to induce the maximum tensile stress at the transverse joint for high and no load transfer. As noted previously, the A-380 produced the highest top tensile stress (LTE=0%). For the high load transfer case, the A-380 aircraft must straddle multiple adjacent slabs to produce the maximum top tensile stress. The positions depicted in Figure 2 (a) and (b) suggest the observed top-down cracking during the NAPTF's tests could have occurred when the two adjacent gears moved

Table 4.

Summary of the Maximum Tensile Stresses at the Top and Bottom of the Central Slab for the Main Landing Gear Loadings ($LTE_X = LTE_Y = 0\%$).

| Aircraft | σ_{tx}^{MAX} (psi) | | Top to Bottom σ_{tx}^{MAX} ratio | σ_{ty}^{MAX} (psi) | | Top to Bottom σ_{ty}^{MAX} ratio |
|----------|---------------------------|-------------|--|---------------------------|------|--|
| | Bottom | Top | | Bottom | Top | |
| A-380 | -473 | -478 | 1.01 | -552 | -356 | 0.64 |
| B-747 | -528 | -414 | 0.79 | -654 | -401 | 0.61 |
| B-777 | -619 | -393 | 0.64 | -455 | -280 | 0.62 |
| MD-11 | -401 | -382 | 0.95 | -650 | -283 | 0.44 |

Table 5.

Summary of the maximum tensile stresses at the top and bottom of the central slab for the main landing gear loadings ($LTE_X = LTE_Y = 85\%$).

| Aircraft | σ_{tx}^{MAX} (psi) | | Top to Bottom σ_{tx}^{MAX} ratio | σ_{ty}^{MAX} (psi) | | Top to Bottom σ_{ty}^{MAX} ratio |
|----------|---------------------------|-------------|--|---------------------------|------|--|
| | Bottom | Top | | Bottom | Top | |
| A-380 | -372 | -258 | 0.69 | -421 | -205 | 0.49 |
| B-747 | -399 | -205 | 0.51 | -456 | -196 | 0.43 |
| B-777 | -490 | -247 | 0.50 | -403 | -219 | 0.54 |
| MD-11 | -366 | -218 | 0.59 | -490 | -213 | 0.44 |

close to the transverse joint, although the magnitude of the top tensile stress case (258 psi) with high load transfer makes it highly unlikely.

Figure 4 shows the results for both the TDT gears of the B-777. For this slab geometry and aircraft gear characteristics, the likelihood of top-down cracking is minimal due to the low ratio of top to bottom tensile stress. The large spacing between the main landing gears is the primary reason why the B-777 aircraft produced lower top tensile stresses in the main landing gear analysis. When all the gears were considered for the B-777 and B-747 aircraft ($LTE=85\%$), the maximum bottom tensile stresses were slightly higher (Table 5) relative to the individual B-747 and B-777 gear analysis (Table 3). The top tensile stresses were also higher for the B-777 full gear analysis and approximately the same for the B-747 individual and full gear analysis.

The critical positions for the MD-11 are illustrated in Figure 5. The maximum tensile stress is located at transverse joint like the A-380 when the gears straddle multiple adjacent slabs. The no load transfer case again produces the largest top tensile stresses. The critical top tensile stress location is almost in the same position as the no load transfer case. This outcome makes sense since the MD-11 gears are not significantly offset in the y-direction.

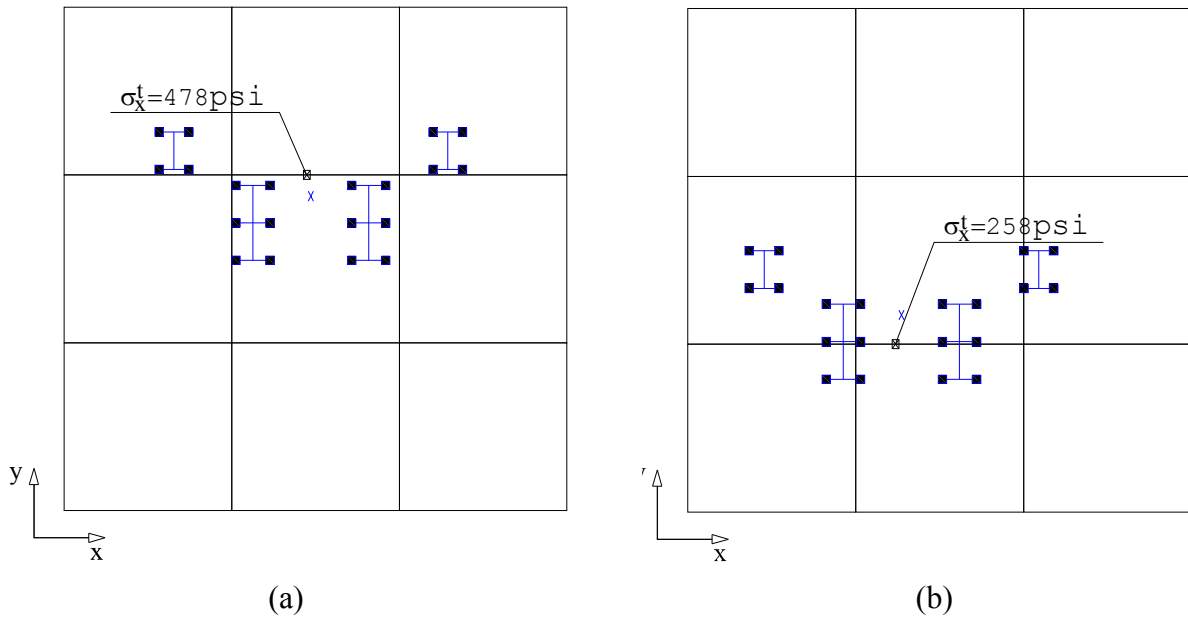


Figure 2. Position of the maximum top tensile stress (σ_t^{MAX}) for the A-380 aircraft for (a) LTE = 0% and (b) LTE = 85%.

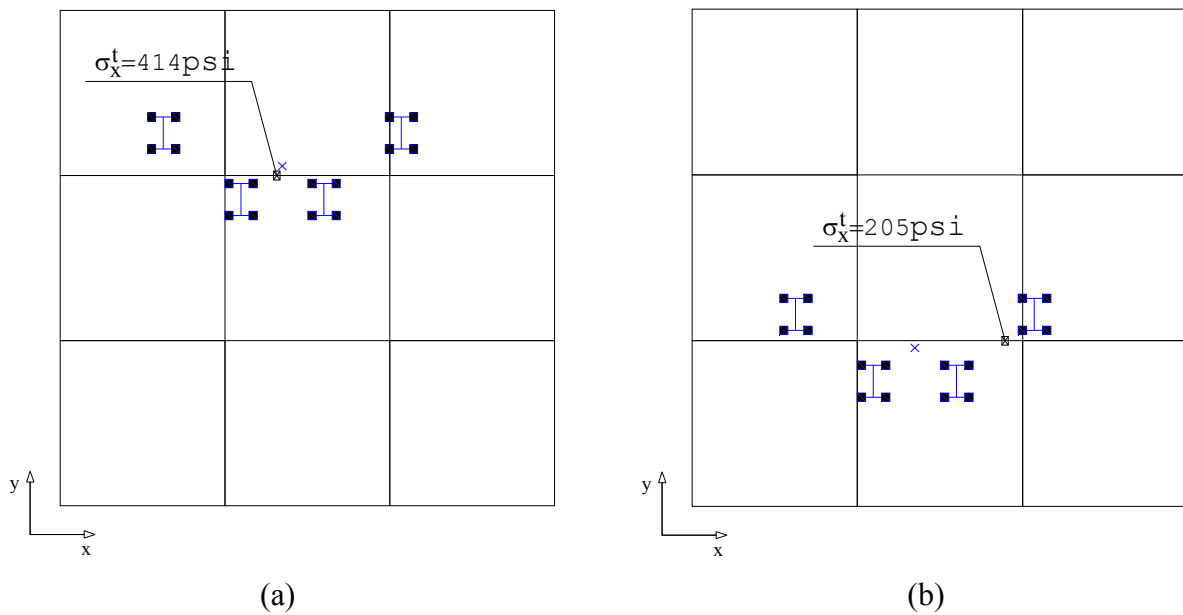


Figure 3. Position of the maximum top tensile stress (σ_t^{MAX}) for the B-747 aircraft for (a) LTE = 0% and (b) LTE = 85%.

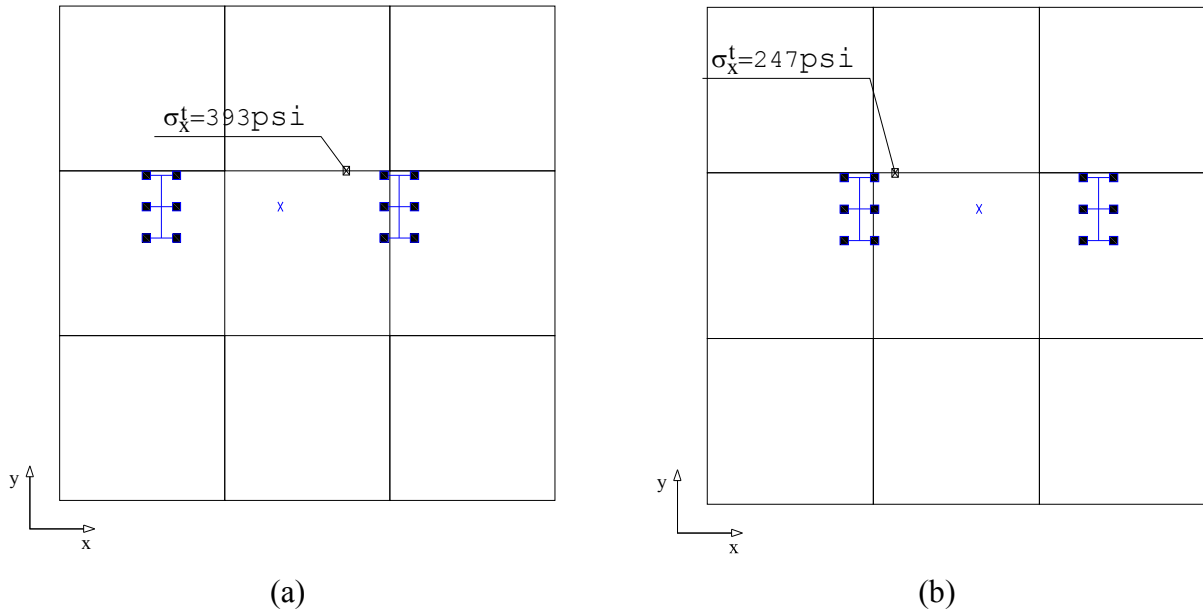


Figure 4. Position of the maximum top tensile stress (σ_t^{MAX}) for the B-777 aircraft for (a) LTE = 0% and (b) LTE = 85%.

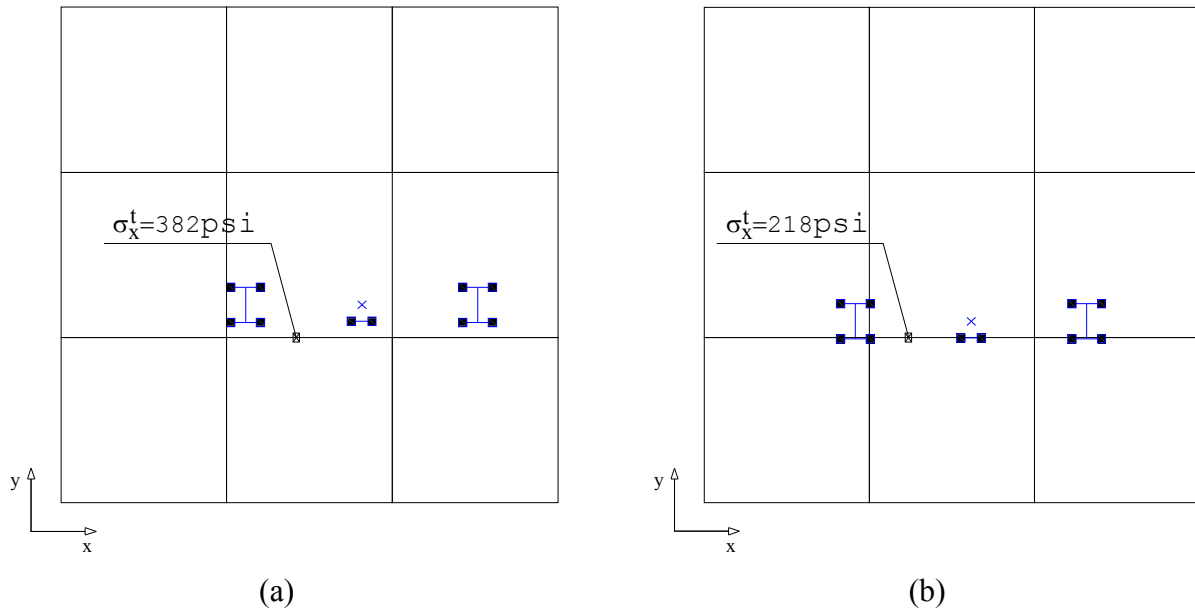


Figure 5. Position of the maximum top tensile stress (σ_t^{MAX}) for the MD-11 aircraft for (a) LTE = 0% and (b) LTE = 85%.

CONCLUSIONS

Recent full-scale testing of airfield rigid pavements resulted in the occurrence of top-down cracking. Two-dimensional numerical simulations were completed on a nine slab airfield rigid pavement system for several different aircraft types. The purpose of this analysis was to determine the likelihood of top tensile stresses approaching the magnitude of bottom tensile stresses in concrete slabs for a no curling assumption. The first finite element runs analyzed 5 individual aircraft gear types (e.g., B-737 dual; B-747, B-757, and B-767 dual tandems; and B-777 triple dual tandem). A second series of analysis loaded the slabs with all the main landing gears of the following aircraft: B-777, B-747, MD-11, and A-380. Two load transfer efficiencies were assumed across the joint (0 and 85 percent) to determine how the stress magnitudes and positions varied for the different aircraft.

As expected, the individual and full gear analysis found the tensile stresses at the bottom of the slab were the most critical. The B-747 and MD-11 produced the greatest tensile stresses at the bottom of the slab for both high and no load transfer, while the main landing gears of the A-380 resulted in the largest top tensile stress for this paper's slab geometry, load per wheel, and pavement layer/material assumptions. The ratio between the top and bottom of the slab tensile stresses were significantly higher for the full gear analysis relative to the individual gear analysis. For the no joint load transfer case, the A-380 had top and bottom tensile stresses in one direction that were approximately the same. The critical top tensile stresses occurred at the transverse joint for all aircraft analyzed which would promote propagation of longitudinal cracks. In all four main landing gear analyses, the critical top tensile stresses were created when the gears straddle multiple adjacent slabs.

This initial finite element analysis has shown consideration of the full aircraft gear is necessary if the top tensile stresses are going to be accurately predicted. If only the individual gear types are analyzed, it is unlikely that top-down cracking will occur unless strength reduction of 50 percent exist at the top of the slab relative to bottom half of the slab. Future work is needed to analyze the effects of 2-D versus 3-D assumptions and confirm the findings presented herein for alternative slab geometry, material properties, aircraft, and with slab curling.

ACKNOWLEDGMENTS

This paper was prepared from a study conducted in the Center of Excellence for Airport Technology, funded by the Federal Aviation Administration under Research Grant Number 95-C-001 and the University of Illinois. The contents of this paper reflect the views of the authors, who are responsible for the facts and accuracy of the data presented within. The contents do not necessarily reflect the official views and policies of the Federal Aviation Administration. This paper does not constitute a standard, specification, or regulation.

REFERENCES

1. Brill, D.R., Hayhoe, G.F. and Ricalde, L., “Analysis of CC2 Rigid Pavement Test Data from the FAA's National Airport Pavement Test Facility,” 7th International Conference on the Bearing Capacity of Roads, Railways, and Airfields, Trondheim, Norway, 2005.
2. Fabre, M.C., Maurice, M.J., Guedon, M.D., Mazars, M.A. and Petitjean, M.J., “A380 Pavement Experimental Programme, Rigid Phase,” Technical Report, 2005.
3. Mahoney, J., Lary, J.A., Pierce, L.M., Jackson, N.C., and Barenberg, E.J., “Urban Interstate Portland Cement Concrete Pavement Rehabilitation Alternatives for Washington State,” Washington State Department of Transportation, Report No. WA-RD 202.1, Seattle, WA, 1991.
4. Smith, K.D., Wade, M.J., Peshkin, D.G., Khazanovich, L., Yu, H.T., and Darter, M.I., “Performance of Concrete Pavements; Volume II—Evaluation of In-service Concrete Pavements,” FHWA-RD-95-110, Washington, DC, 1996.
5. Harvey, J.T., Roesler, J.R., Farver, J. and Liang, L., “Preliminary Evaluation of Proposed LLPRS Rigid Pavement Structures and Design Inputs,” Final Report, FHWA/CA/OR-2000/02, University of California-Berkeley, Pavement Research Center, Richmond, CA, 2000.
6. Heath, A.C. and Roesler, J.R., “Top-Down Cracking of Rigid Pavements Constructed with Fast Setting Hydraulic Cement Concrete,” *Transportation Research Record 1712*, TRB, National Research Council, Washington, D.C., pp. 3-12, 2000.
7. Beckemeyer, C.A., Khazanovich, L., and Yu, H.T., “Determining the Amount of Built-in Curling in JPCP: A Case Study of Pennsylvania I-80,” *Transportation. Research. Records.*, 1809, 85-92, 2002.
8. Heath, A.C., Roesler, J.R., and Harvey, J.T., “Modeling Longitudinal, Corner and Transverse Cracking in Jointed Concrete Pavement,.” *International Journal of Pavement Engineering*, 4(1), 51-58, 2003.
9. Hiller, J.E. and Roesler, J.R., “Determination of Critical Concrete Pavement Fatigue Damage Locations Using Influence Lines,” *ASCE Journal of Transportation Engineering*, Vol. 131, No. 8, pp. 599-607, 2005.
10. Rao, S. and Roesler, J.R., “Nondestructive Testing of Concrete Pavements for Characterization of Effective Built-In Curling,” *ASTM Journal of Testing and Evaluation*, Vol. 33, No. 5, pp. 356-363, 2005.
11. Rao, S. and Roesler, J.R., “Characterizing Effective Built-In Curling from Concrete Pavement Field Measurements,” *ASCE Journal of Transportation Engineering*, Vol. 131, No. 4, pp. 320-327, 2005, 2005.
12. Hayhoe, G.F., “Traffic Testing Results from the FAA's National Airport Pavement Test Facility,” Proceedings of the 2nd International Conference on Accelerated Pavement Testing, University of Minnesota, Minneapolis, Minnesota, USA, 2004.
13. Brill, D., “Performance Modeling of Rigid Airports Pavements Incorporating Full-Scale Test Data from the FAA National Airport Pavement test facility”. 6th International DUT – Workshop on Fundamental Modelling of Design and Performance of Concrete Pavements, Belgium, September, 2006.
14. Guo, E. H., “Fundamental Modeling of Curling Responses in Concrete Pavements,” 6th International Workshop on Fundamental Modelling of Design and Performance of Concrete Pavements, Belgium, September, 2006.

15. Rao, S., "Characterizing Effective Built-In Curling and its Effect on Concrete Pavement Cracking," Ph.D thesis, University of Illinois, Urbana, IL, 2005.
16. Fabre, M.C. and Balay, J.M., "A380 Pavement Experimental Programme, Rigid Tests," FAA Pavement Workgroup Meeting, 2005.
17. McCullough, B.F. and Dossey, T., "Considerations for High-Performance Concrete Paving: Recommendations from 20 Years of Field Experience in Texas," *Transportation Research Record 1684*, TRB, National Research Council, Washington, D.C., pp. 17-24, 1999.
18. Khazanovich, L., "Structural Analysis of Multi-Layered Concrete Pavement Systems," Ph.D. Dissertation, University of Illinois, Illinois, USA, 1994.